RESEARCH ARTICLE

The role of natural rubber latex nanoparticles in tissue engineering

Masami Okamoto¹

¹ Advanced Polymeric Nanostructured Materials Engineering, Graduate School of Engineering, Toyota Technological Institute, 2-12-1 Hisakata, Tempaku, Nagoya 468 8511, Japan

OPEN ACCESS

ABSTRACT

Natural rubber latex is derived from the lactiferous sap of the *Hevea brasiliensis* (para rubber tree) and has been used in traditional medicine due to its bioactive compounds. There are over 35,000 species of plants that produce latex. Recently, NRL has shown promise in tissue engineering for the replacement and regeneration of various tissues, such as skin, eardrums, bones, and dental alveoli. This presents a unique opportunity to repair or replace failing organs or tissues. This review highlights the current development of Natural rubber latex in tissue engineering, and identifies importance for investigation on cytotoxicity of Natural rubber latex nanoparticles. In addition, promising results regarding the current challenges and perspectives of Natural rubber latex-based tissue engineering is discussed.

Keywords: Natural rubber latex; Nanoparticles; Tissue engineering; Cytotoxicity, Biocomposites

1. Introduction

Latex is widely distributed among plants, with over 35,000 lactiferous plant species, containing bioactive compounds used in folk medicine as traditional sophisticated systems[1, 2]. Until now, only a mere 1% of plant species have been studied for their pharmacological potential, meaning the majority remains an unknown realm of medicinal systems. There is great anticipation for discovering new therapeutic compounds from latex, holding promising pharmacological possibilities.

Natural rubber (NR), obtained by coagulating NR latex (NRL), is a high molecular weight polymer. Currently, over 90% of NRL comes from a single species, *Hevea brasiliensis* (rubber tree)[3]. NR and NRL are primarily used in various traditional industrial products such as gloves, condoms, balloons, medical devices, and tires. Regarding NRL, its applications have been continually expanding into tissue engineering. Recently, several promising results have been reported regarding the fabrication of replacement and regenerative tissues using NRL derived from *H. brasiliensis*[4-8].

In particular, wound healing in cutaneous tissues, eardrum replacement, bone regeneration, and dental alveolus replacement offer unique approaches to repair or replace failing organs or tissues[5,8]. Latex biomembranes (LBM) derived from H. brasiliensis demonstrate a tendency to serve as cost-effective alternatives to conventional treatment methods, exhibiting structural properties and promoting angiogenesis for tissue healing and serving as biomaterials[9].

Previous studies have been paid little attention to pharmacological potential activity of NRL as nanoparticle. The reason behind this is well explored as allergic problems in some sensitive individuals, which cause immediate hypersensitivity, mediated by immunoglobulin E (IgE) antibodies to specific (high-sulfur) proteins in the latex. On the one hand, however, the prevalence of latex allergy in population is believed to be very low[10]. In this review we summarize the current development of NRL in tissue engineering and regenerative medicine, and identify importance for investigation on cytotoxicity of NRL nanoparticles. In addition, we provide promising research regarding the current challenges and perspectives of NRL-based tissue engineering.
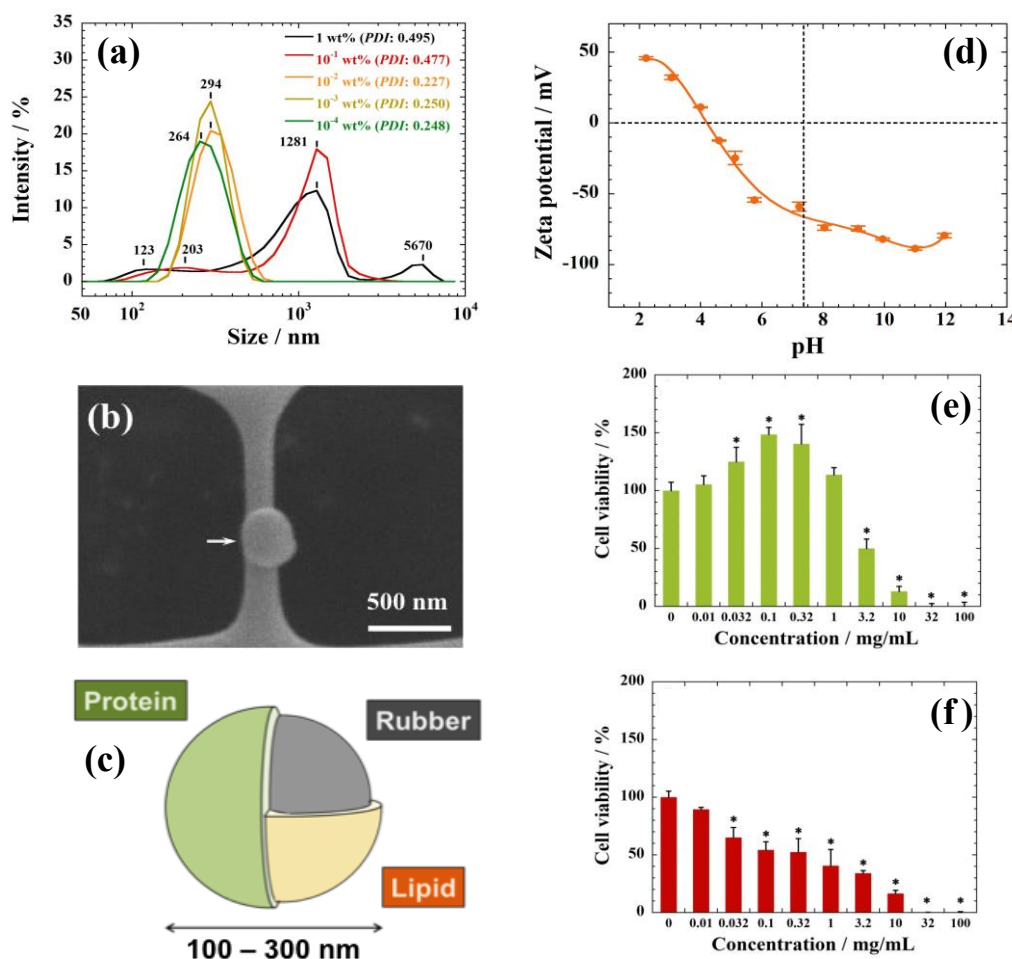

Fig. 1. (a) Size distribution of NRL nanoparticles in water at various concentrations ranging from 10^{-4} to 1 wt% as determined by the polydispersity index at pH 7.4. (b) Microscopic images showing individual NRL nanoparticles (at concentrations of 10^{-4} to 1 wt%). (c) The top surface is covered with a thin layer (~ 20 nm thick) of proteins and phospholipids. The proteins possess both positively and negatively charged species, resembling amino acid molecules.
(d) Zeta potential of NRL nanoparticles in water (at a concentration of 0.01 wt%) as a function of pH. Results are expressed as mean $\pm$ standard deviation (SD). (e) Cell viability measured by the WST-8 assay using MC3T3-E1 cells after incubation with NRL nanoparticles at different concentrations for 24 hours. Data are presented as mean $\pm$ standard deviation (SD). (f) Cell viability measured by the WST-8 assay using A549 cells after incubation with NRL nanoparticles at different concentrations for 24 hours. Data are presented as mean $\pm$ standard deviation (SD). Note: * indicates $p < 0.05$ compared to the control group.
(Copyright 2017. Reproduced from ref. 11, 13).

2. Structure and characteristics of NRL nanoparticles

The primary particle size of NRL falls within the range of 100 to 300 nm[11], making it a promising nanomaterial for applications in pharmaceuticals, tissue engineering, regenerative medicine, and other biotechnological fields (Figure 1a, b). Nanoparticles are typically taken up through endocytosis. Particle sizes ranging from 20 to 200 nm are suitable for drug delivery applications based on in vitro studies[11]. Upon increasing the concentration up to 1.0 wt.%, the formation of clustered nanoparticles with a size around 1.0 wt.% is observed. A polydispersity index of approximately 0.5 reveals a size range of 1300–5000 nm, indicating that the nanoparticles are not electrostatically stable due to weak ionic characteristics at pH 7.4.

On the surface, there is a thin layer with 20 nm thick of proteins and phospholipids. The proteins contain both positively and negatively charged species, resembling amino acid molecules. NRL nanoparticles possess variable surface charges dependent on the pH of the surrounding solution, as the amino acid residues gain or lose protons accordingly. As a result, the net negative charge is reaching approximately –70 mV at pH 7.4 (showed by the dashed line). The zero-charge point is at pH 4.1 (Figure 1c, d)[11,12].

The fractionated NRL have previously been characterized the substances in latex in the largest amounts of proteins, lipids and inorganic salts[11]. The fractionated NRL by ultra-centrifuge is composed of three constituents: (1) rubber component (94 wt.%) attributed to *cis*-1,4-polyisoprene; (2) intermediate phase (5.8 wt.%) corresponding to dissolved components in water, exhibits adsorbed proteins together with adsorbed phospholipids on the NRL surfaces; (3) sediment (0.2 wt.%) is non-rubber constituents such as inorganic ions and sterol glycosides[11].

The sediment contains lutoid organelles that perform biochemical function, such as allergic reactions. The intermediate phase is related to different biological properties. One of the first application of the intermediate phase in the clinical area is the prevention of liver cancer cells by non-apoptotic cell death[12]. Research on the anticancer activity of NRL utilizing the physiological properties of natural compounds has gained significant attention. Regarding this, several studies have evaluated the safety and potential adverse effects on the biological system[13,14]. Furthermore, the underlying mechanisms behind the interaction with living cells are being investigated in the literature. To fully understand the hazards associated with NRL particles, further information regarding their potential cytotoxicity and the toxicological mechanisms is necessary.

3. Cytotoxicity of NRL nanoparticles

Recently, Okamoto et al. demonstrated the cell compatibility of latex on cultured human lung carcinoma (A549) and mouse preosteoblast (MC3T3-E1) cells in vitro. MC3T3-E1 cells showed high sensitivity to NRL concentration, exhibiting increased metabolic activity and dehydrogenase activity at concentrations below 10.0 µg/mL. When the concentration exceeded 10.0 µg/mL, NRL nanoparticles improved cell viability of MC3T3-E1 cells ranged from 130 to 150% compared to the control (Figure 1e).

By contrast, NRL particles were found to be toxic to A549 cells, with cell viability being less than 60% at a concentration of 100 µg/mL (Figure 1f). Administration of NRL particles effectively inhibited the proliferation of A549 cells within one day. The estimated half-maximal inhibitory concentration (IC_{50}) values at the maximum inhibitory concentration ranged from 10 µg/mL to 10 mg/mL, with 330 ± 20 µg/mL for A549 cells and 3.97 ± 0.1 mg/mL for MC3T3-E1 cells [11]. Their data demonstrated that the addition of 1.0 mg/mL of NRL nanoparticles to the cell culture did not induce cell death in the tested MC3T3-E1 cells. When applying NRL nanoparticles for anticancer drug delivery, exposure of the NRL nanoparticles to the living tissue is anticipated[14]. Ongoing experiments aim to elucidate the underlying reasons for this observation. This behavior will be further discussed based on the relationship with the endocytosis process of NRL nanoparticles into the cells. This report contributes to advancing the research on NRL nanoparticles, which are highly promising bio-nanoparticles with potential as anticancer agents to induce an apoptotic cell death. The researchers may expect that using NRL as an anticancer agent could mitigate severe side effects on normal (healthy) human cells.

Floriano's group reported the cytotoxicity of NRL from different clones of *H. brasiliensis*[7]. *H. brasiliensis* exhibits significant genetic diversity. The RRIM 600 clone is the most widely used clone in rubber production in Brazil. When NRL membranes prepared without the use of ammonia in the latex extraction process were utilized, it was demonstrated that the proliferation of fibroblast cells (NIH3T3) was observed after a 3-day incubation period, suggesting the bioactive behavior of the RRIM 600 clone towards healthy cells.

4. Potential Target Applications in Tissue Engineering

Normal cells are optimally supported by interaction with a soft and/or stiff matrix with various elastic modulus ranged from 50 Pa to 2 GPa (Figure 2)[15]. Compliant tissue such as lung exhibit low stiffness (300 Pa), whereas tissues exposed to high mechanical loading, such as bone or skeletal muscle exhibit high stiffness with four orders of magnitude greater (10^4–10^6 Pa). By contrast, the blood and mucus exhibit very low modulus of 50 Pa[15]. Natural living tissue including cells have a genetically programed capacity for self-repair.

Consequently, natural tissue can adapt to their physiological environment (microenvironment). The interface between NRL-based implant and its host tissue is especially susceptible to stress. Mismatch either biomechanical factor can lead to interfacial deterioration and transformation of normal cells to tumour cells become hyper-responsive to matrix elasticity.
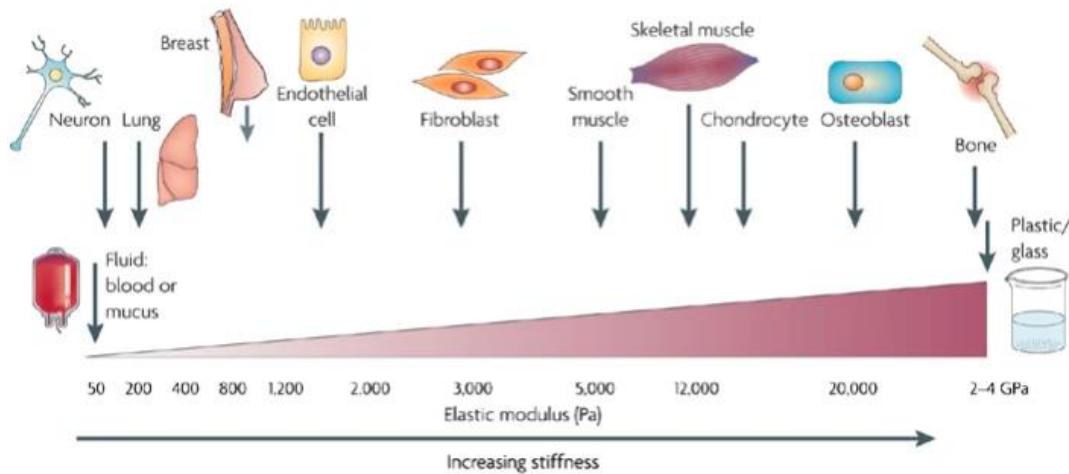
Fig. 2. Cells are tuned to the materials properties of their matrix.
All cells, including those in traditionally mechanically static tissues, such as the breast or the brain, are exposed to isometric force or tension that is generated locally at the nanoscale level by cell–cell or cell–extracellular matrix interactions and that influences cell function through actomyosin contractility and actin dynamics. Moreover, each cell type is specifically tuned to the specific tissue in which it resides. The brain, for instance, is infinitely softer than bone tissue. Consequently, neural cell growth, survival and differentiation are favored by a highly compliant matrix. By contrast, osteoblast differentiation and survival occur optimally on stiffer extracellular matrices with material properties more similar to newly formed bone. We can emphasize the critical association between tissue phenotype and matrix rigidity.
(Copyright 2009. Reproduced from ref. 15).

4.1. BONE REGENERATION

In 2014, Floriano's group reported a new discovery where LBM (latex biomembrane) prepared from RRIM 600 and IAN 873 clones without the use of ammonia was transplanted subcutaneously in rabbits, resulting in favorable biocompatibility of the membranes from these clones[7]. The membranes derived from RRIM 600 and IAN 873 clones induced greater cell proliferation, suggesting enhanced biological activity. As seen in Figure 3, the underlying tissue beneath the implant exhibited a normal appearance with no signs of necrosis or ulceration. Tissue sections showed minimal presence of inflammatory cells and no fibrotic capsules were observed (Figure 3c). Subsequently, Kinoshita's group reported results related to bone repair[16]. This process is associated with substances naturally present in NRL nanoparticles and stimulates not only angiogenesis, a critical requirement for bone repair, but also cell adhesion and formation of extracellular matrix[10,17].
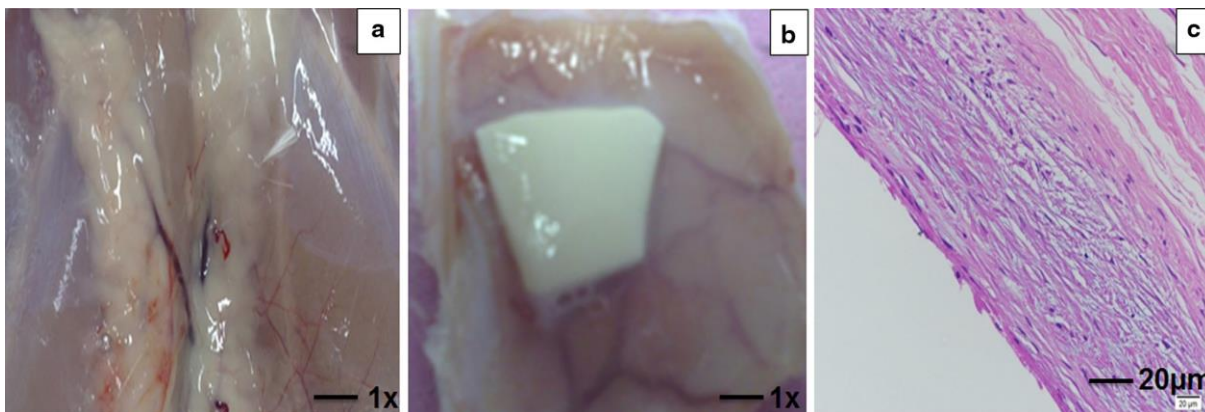

Fig. 3. (a) Macroscopic image of the surgical site of the NRL membrane derived from clone IAN 873, taken 1 month after surgery. The implanted area is shown.
(b) Image showing the removed portion of the NRL membrane.
(c) Histological analysis of the surgical site, indicating the tissue composition.
(Copyright 2014. Reproduced from ref. 7).

Two bone defects (10 mm diameter) were surgically created in the coronal region of the skulls of 30 adult male New Zealand rabbits. The defects were treated with guided bone regeneration (GBR) using either NRL (prepared without the use of ammonia in the latex extraction process) or polytetrafluoroethylene (PTFE; as the gold standard control) membranes. Microscopic analysis revealed that at 7 days, the defects treated with both membranes showed new bone formation at the edges filled with blood clots, while at 20 days, the defects were primarily filled with fibrous connective tissue. After 60 days, the defects covered with LBM demonstrated significantly larger areas of bone formation compared with the other groups.

Furthermore, hypersensitivity reactions of the bone tissue

to LBM and PTFE membranes were investigated in an additional 6 rabbits. The animals underwent the same surgical procedure for a 10 mm diameter bone defect treated with either LBM or PTFE. After 53 days, a second surgery was performed to create a second defect, which was then treated with the same type of membrane used in the initial surgery. After 7 days, the animals were euthanized, and the samples were analyzed. No differences were observed between the LBM samples collected from sensitized animals and non-sensitized animals, as well as between the PTFE samples.

The morphological characteristics of the sensitized samples collected 7 days after the placement of the second LBM and PTFE membranes (Figure 4A) were similar to the samples that were not sensitized beforehand. Images highlighting the defect edges, which indicate new bone formation characterized by cement lines, are shown in Figure 4B[16]. Therefore, the results demonstrate that the latex membrane exhibits performance comparable to the PTFE membrane and that LBM induces higher levels of bone formation. Both LBM and PTFE membranes did not induce hypersensitivity reactions in the bone tissue.
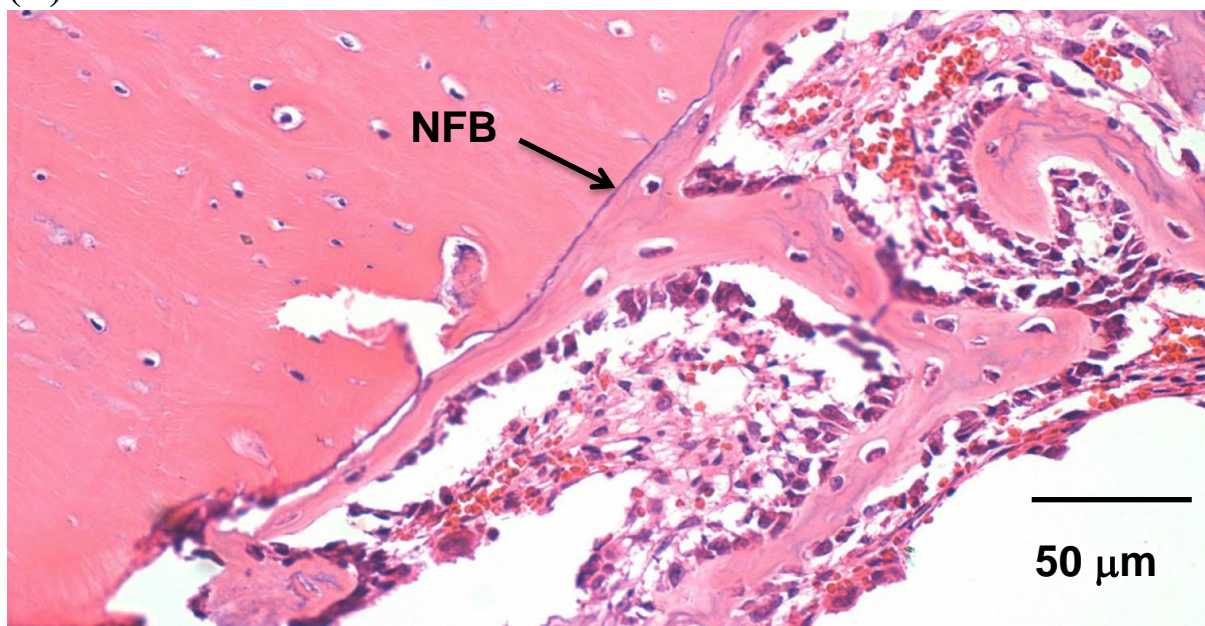
(A)
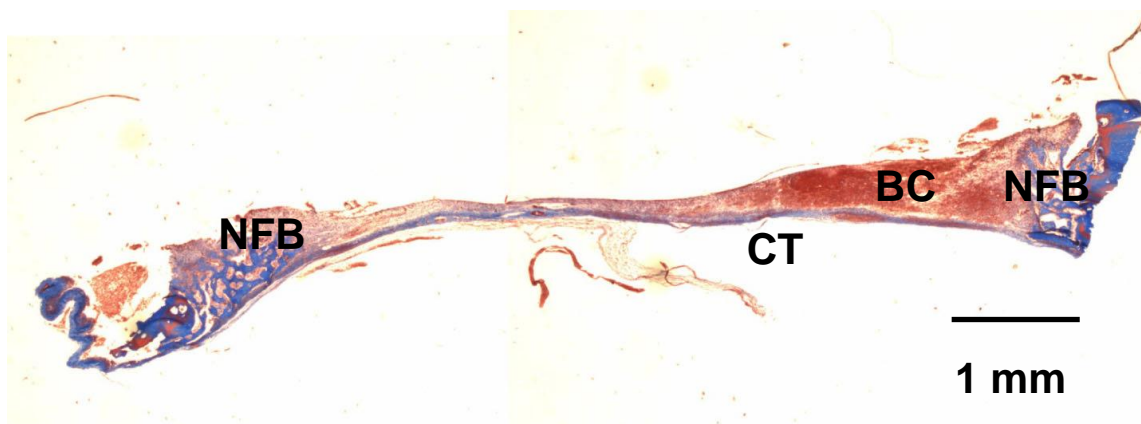
(B)

Fig. 4. (A) Microscopic images of the 7-day samples treated with NRL after a 53-day sensitization period. The pattern is similar to that of the non-sensitized case, with the defect filled with a thin layer of connective tissue (CT) and a blood clot (BC). At the edge of the defect, newly formed bone (NFB) can be observed (2x, Masson's trichrome staining).
(B) The edge of the defect (40x, hematoxylin and eosin staining) showing the cement line (arrow) characterizing the newly formed bone (NFB).
(Copyright 2014. Reproduced from ref. 16).

To match the interface between NRL nanoparticles and its host tissue, Furuya et at. examined osteogenic differentiation, as well as expressions of multiple MC3T3-E1 osteoblast proteins using NRL and NRL-hydroxyapatite (HA) nanoparticles[18]. Neither NRL nor NRL-HA exhibited toxic effects for MC3T3-E1 cells at concentrations of 0.01 to 5 mg/mL (viability in the range of 100 to 150%). The results indicated the NRL nanoparticles as promising to be used in bone tissue engineering. It has also been found that

for the NRL-HA composite particles, where HA (the main mineral component of bone) was deposited on the surface of the NRL particles, there was an improvement in their biocompatibility, stimulating osteoblasts differentiation. Besides, the results of the gene analysis revealed that Okamoto's group concluded that the NRL particles are bio-materials that can be applied in biotechnology engineering.

4.2. VASCULARIZATION

In cases of larger bone defects, bone conduction alone is not sufficient, and additional components are necessary to achieve healing. Therefore, current efforts are focused on the development of composite systems that combine bone substitute materials with active molecules for bone regeneration, aiming to improve the osteogenic capacity[19]. Bone morphogenetic proteins are among the most efficient molecules in stimulating bone formation induction[20,21]. However, for successful bone repair, early-stage angiogenesis is also crucial, particularly in cases of larger defect sizes.

Delivery of angiogenic factors, replenishment of endothelial cells, and stimulation of functional vascular network formation are critical events that occur during the early stages of bone repair[22]. Therefore, angiogenesis precedes bone formation and determines the efficiency of bone healing. Several clinical evidence has reported the stimulation of wound healing, promotion of blood circulation, and reestablishment of vascular neovascularization in chronic wounds, such as diabetes and pressure ulcers, treated with LBM[23]. According to Frade et al.[24], the presence of growth factors in latex induces angiogenesis and promotes the repair of diabetic and venous ulcers, leading to improved local neovascularization and subsequently inducing re-epithelialization.

In 2010, protein fractions (F1) extracted from natural latex showed promising results in preclinical studies regarding angiogenic stimulation and tissue repair[6,25]. Shortly after, Almedia's group presented different types of latex obtained from *Hancornia (H.) speciosa*, which is used in folk medicine for the treatment of several diseases[8]. Biocompatibility was evaluated through cytotoxicity and genotoxicity tests on mouse fibroblast cells, as well as angiogenic properties using the chicken chorioallantoic membrane (CAM) assay model. The physicochemical results indicated that the structure of H. speciosa latex biomembrane is highly similar to that of *H. brasiliensis*. The CAM test demonstrated the efficient ability of H. speciosa latex in tissue neovascularization. Histological analysis was consistent with the results obtained from the CAM assay. Their findings indicate that water-extracted latex obtained from *H. speciosa* showed significant angiogenic activity without exerting cytotoxic or genotoxic effects on living systems. The addition of ammonia did not have a significant impact on the structure of the biomembrane but resulted in decreased cell viability and demonstrated notable genotoxic effects.

Figure 5 shows various images of CAM, and the three groups (LW, LA, and RE) treated with latex exhibited the formation of more and thicker blood vessels compared to the negative control and dexamethasone groups (W and DE). Figure 5 also demonstrates the measurement of neovascularization obtained from CAM image analysis. For water and ammonia-extracted H. speciosa latex, the average percentages of neovascularization were 21.23 ± 1.62 and 20.27 ± 1.35, respectively. Regederm® (positive control) showed a value of 20.40 ± 3.21. The negative control (water) had a value of 9.18 ± 2.27, and dexamethasone had a value of 6.65 ± 2.37. H. speciosa latex exhibited a significant increase in the formed vascular network compared to the negative control ($p < 0.05$) and the inhibitor ($p < 0.05$). No significant difference was observed between H. speciosa latex and the positive control. This study contributes to the understanding of the potential of *H. speciosa* latex as a source of new plant-based medicines.
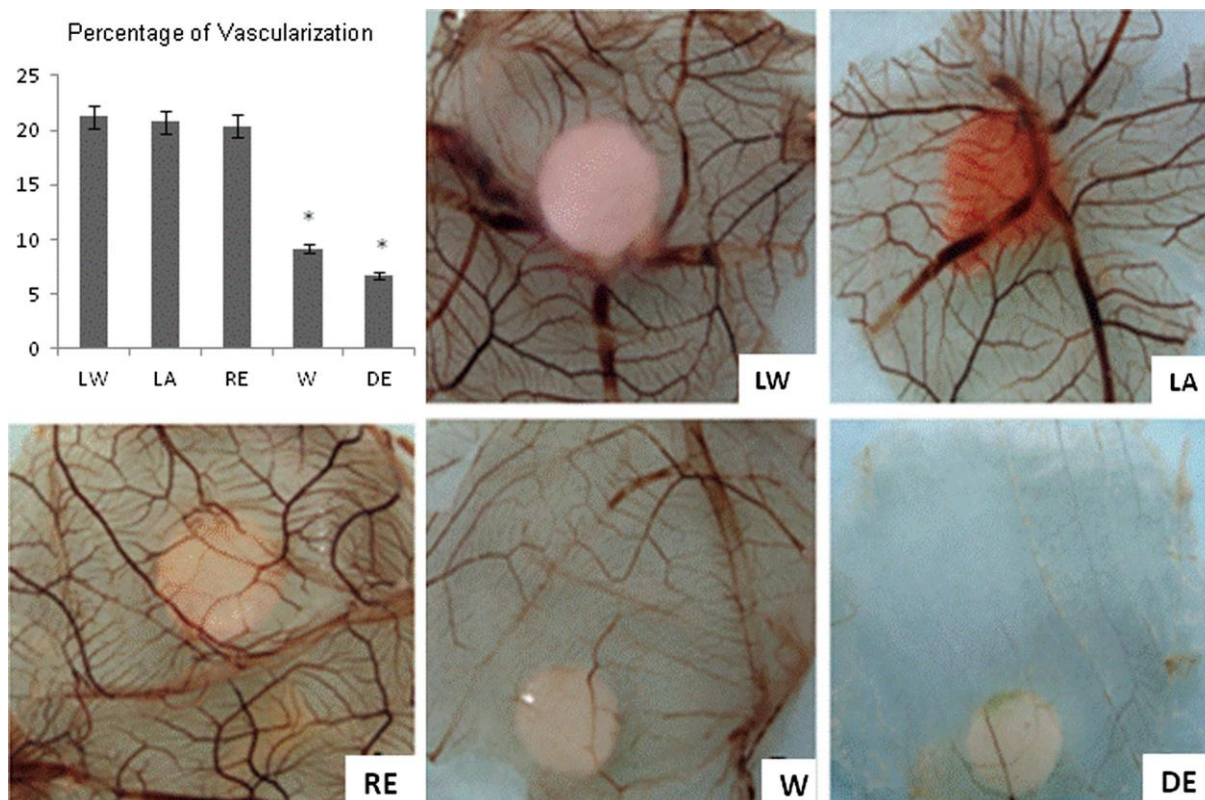

Fig. 5. Various CAM (chorioallantoic membrane) images: LW (*H. speciosa* in water). LA (*H. speciosa* in ammonia); RE (Regederm®, positive control); W (water, negative control) and DE (dexamethasone, angiogenesis inhibitor). The angiogenesis measured from the image analysis is also displayed for the different groups analyzed. * p<0.05
(Copyright 2014. Reproduced from ref. 8).

4.3. CARTILAGE TISSUE COMPOSITES

Due to the challenging nature of self-healing in cartilage injuries, cartilage regeneration has become a highly complex topic in tissue engineering and regenerative medicine[26,27]. The chondrogenic potential of NRL nanoparticles on human mesenchymal stem cells (hMSCs) has been reported[28,29]. For in vitro chondrogenesis in hMSCs with NRL administration, the effective gene expression was confirmed through chondrogenic gene expression analysis. Okamoto's group achieved the first successful creation of a cartilage/NRL bio-composite material through hMSC spheroid formation, demonstrating a mechanically stable structure with a hard surface architecture within the spheroids upon NRL nanoparticle administration.

The viability of hMSCs under normoxic condition indicates very sensitive to the NRL nanoparticle concentration, accompanied with high metabolic and dehydrogenase activity of the cells at concentration of less than 0.1 mg/mL (Figure 6a)[28,29]. Beyond concentration of 0.1 mg/mL, NRL nanoparticles enhance hMSCs and viability in the range of 130–150% in comparison with the control within 24 h. The estimated IC_{50} values are 1.7 mg/mL for hMSCs in the range of 10 μg/mL–10 mg/mL. With increasing concentration up to 1.0 mg/mL, a significant vitality reduction is not observed in comparison with the control for the detection of living cells by WST-8 assay. Under hypoxic condition, hMSCs exhibit no toxic effects and are not sensitive to NRL nanoparticles at concentration up to 1.0 mg/mL. The results demonstrate higher biocompatibility of the NRL nanoparticles without a significant vitality reduction for hMSCs under both normoxic and hypoxic conditions. In hypoxia, the estimated IC_{50} values are 1.55 mg/mL for hMSCs in the range of 10 μg/mL–10 mg/mL.
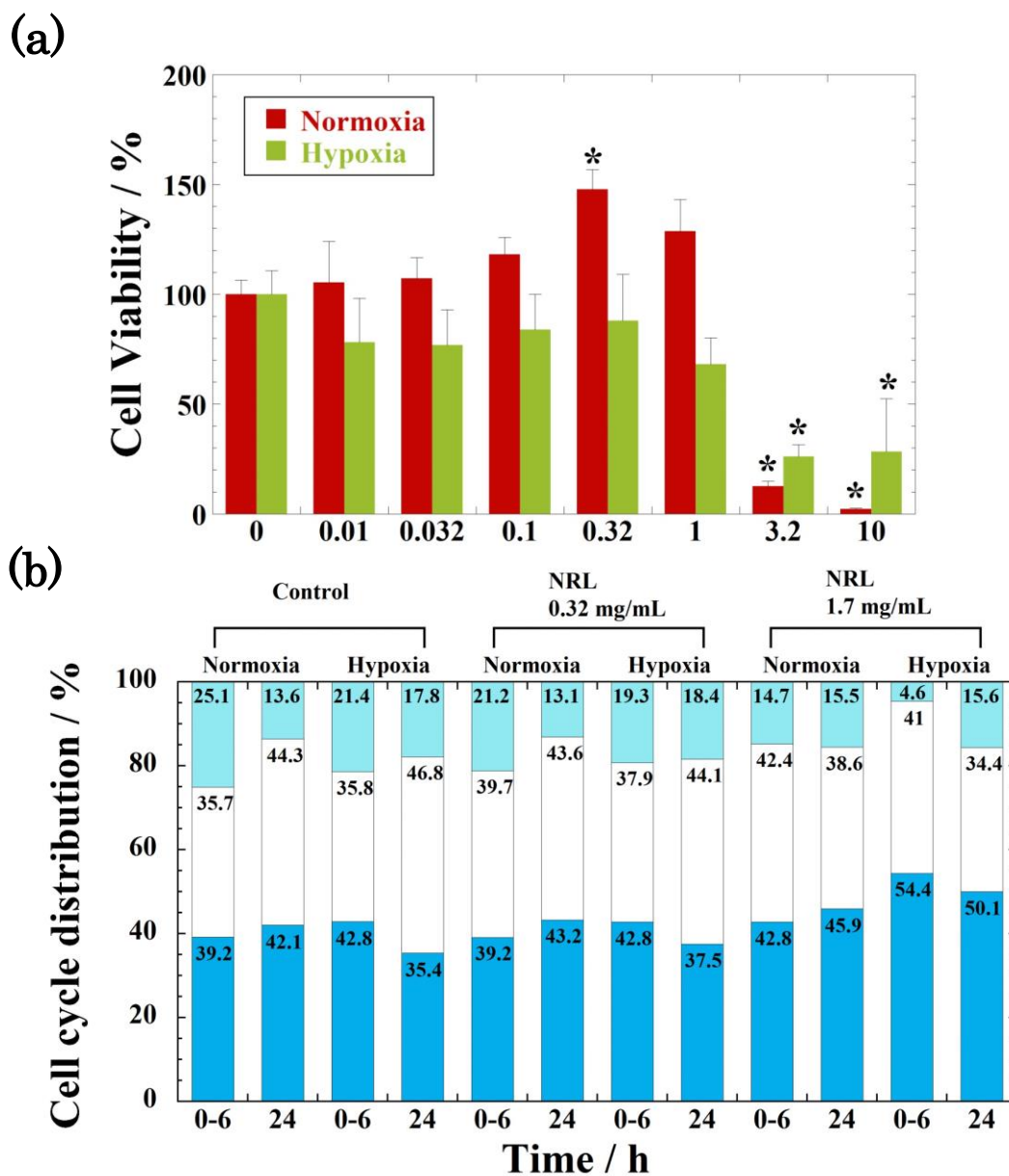

Fig. 6. (a) Effect of oxygen concentrations on cell viability as measured by WST☐8 assay using hMSCs after 24 h of incubation with NRL nanoparticles of different concentrations. Data were expressed as mean ±S.D. (*n*=4). Note: * indicates *p* < 0.05 compared with control. (b) Effect of oxygen concentrations on cell cycle distribution of hMSCs after without treatment (control), treated with NRL nanoparticles of 32 μg/mL and of 1.7 mg/mL (equal to IC_{50} in normoxia for hMSCs) in G_0/G_1 (dark colors), S (white), and G_2/M (light colors) for 0–24 h.
(Copyright 2020. Reproduced from ref. 29).

The cell cycle has been examined with the focus on the cellular proliferation. For better understanding of the

proliferation state the cell cycle distribution is shown in Figure 6b. The cell proliferation is controlled by different phases such as the G_0/G_1 (containing two copies of each chromosome), S (synthesis of chromosomal DNA), G_2/M (doubled chromosomal DNA) phases. Under normoxic condition, the hMSCs exhibits no observed notable difference in distribution from 6 to 24 h, as compared to that of control under the cells exposed to NRL concentration of 0.32 mg/mL. For the cells incubated with IC_{50} value (1.7 mg/mL), the prolonged G_0/G_1 phase for 24 h incubation indicates the presence of cell death such as apoptosis[11]. In addition, the small increment of the fraction of cells with NRL nanoparticles (1.7 mg/mL) is found in the G_2/M phase. In hypoxia, this condition shows some significant effect on the prolonged G_0/G_1 phase for 24 h incubation with NRL nanoparticles (1.7 mg/mL, which is near IC_{50} in hypoxia) in comparison with the cell cycle at concentration of 0.32 mg/mL ($< IC_{50}$). It is clear from these cell cycle distributions that the almost no effect of suppression on the proliferation for hMSCs seems to be different due to the significant difference in cytotoxicity accompanied by NRL concentration in the medium. Their data show that the addition of even as much as 1.0 mg/mL of NRL nanoparticles in cell culture did not kill tested hMSCs. The potential application NRL nanoparticles to biological tissue is expected when one applies NRL nanoparticles as an additive for the regenerative cartilage tissue.

They have shown details of the gene expression of HIF-1α, SOX9, aggrecan, collagen type-II (Col-II), collagen type-I (Col-I), and runt-related transcription factor 2 (Rux2), which are essential for the chondrogenesis[28,29]. The expression level of SOX9, aggrecan and Col-II are high in the spheroid, indicating that chondrogenic differentiation is successfully induced by the administration of NRL nanoparticles in hypoxia.

The most widely used 3D model is a conglomerate of cell aggregates formed under non-adhesive conditions, which can replicate the dimensions of the microenvironment[30]. Figure 7 presents an overview of the cross-section of cartilage (spheroids) after 21 days of cultivation under low oxygen conditions. Histological examination of these specimens using hematoxylin and eosin (HE) staining revealed heterogeneous spatial cell distribution throughout all the specimens (Figure 7a–d)[29]. The cartilage cells exhibited a rounded morphology, likely due to the low oxygen environment, in the outer regions of the spheroids. In the central regions of the spheroids, cartilage tissue based on type II collagen (Col-II) was matured throughout all the specimens. Bright-safranin-O staining indicated the abundant presence and uniform distribution of glycosaminoglycans within the spheroids (Figure 7e–h). No differences were observed in the histological examination across all the specimens.
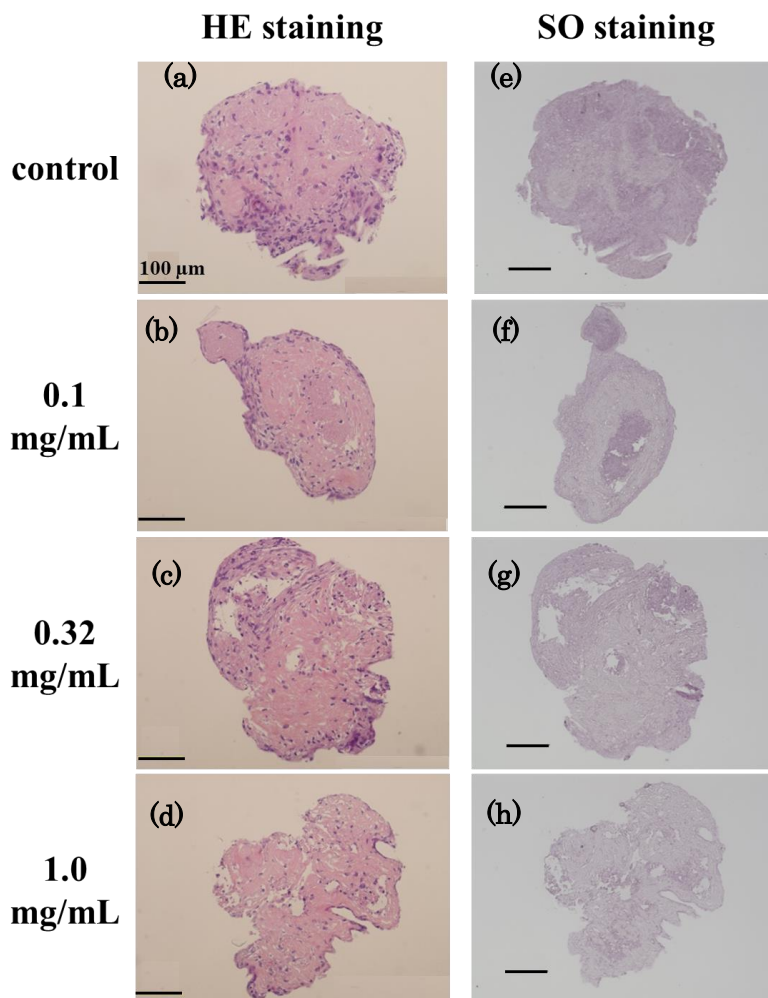

Fig. 7. Representative microscopic images of internally migrated type-II collagen and glycosaminoglycans in control and NRL-loaded spheroids on day 21 of culture under hypoxic conditions: (a) – (d) Hematoxylin-stained cell nuclei (blue) and Hematoxylin-eosin stained type-II collagen (red); (e)–(h) Safranin O-stained glycosaminoglycans (red). The bar represents 100 µm. (Copyright 2020. Reproduced from ref. 29).

The cartilage cell spheroids in phosphate-buffered saline were subjected to atomic force microscopy (AFM) indentation to detect the heterogeneity of stiffness[29]. Maps of adhesion and Young's modulus, with a size of 20 x 20 μm^2, were composed of these indented regions (Figure 8a and 9a). For spheroids (approximately 600 μm) cultured with NRL nanoparticles at three different concentrations (1.0, 0.32, and 1.0 mg/mL), the obtained topographic images exhibited smoother surface morphology compared to the control[29]. The heterogeneity of stiffness was also detected through AFM indentation. In the initial stages of deformation (corresponding to the approach curve), the composition of the surrounding surface of the spheroids was carefully monitored. The observed heterogeneous structure revealed significant deformability in the unloading force curve, indicating a substantial capacity for deformation.

The histogram of elastic modulus for spheroids (control) cultured without NRL nanoparticles showed a distribution ranging from 4 to 60 kPa, with an evaluated mean elastic modulus of 6.7 kPa based on the Weibull distribution curve (upper panel of Figure 8b). Interestingly, when comparing the stiffness of spheroids filled with NRL at a concentration of 0.32 mg/mL, surface heterogeneity was observed, with the spheroids exhibiting higher elastic modulus (54.1 kPa) and a broader distribution of elastic modulus ranging from 4 to 300 kPa (third panel of Figure 8b), indicating the effect of NRL nanoparticle administration on hMSC chondrogenic differentiation. This finding suggests a significant contribution of NRL nanoparticle dispersion in surface structures to cartilage formation. The elastic modulus of NRL was measured to be approximately 1 MPa, which is much higher than the elastic modulus of cartilage tissue[31]. However, the modulus mismatch between cartilage and NRL does not occur. Furthermore, spheroids with an NRL concentration of 1.0 mg/mL showed an overall decrease in stiffness (6.2 kPa) (lower panel of Figure 8b).
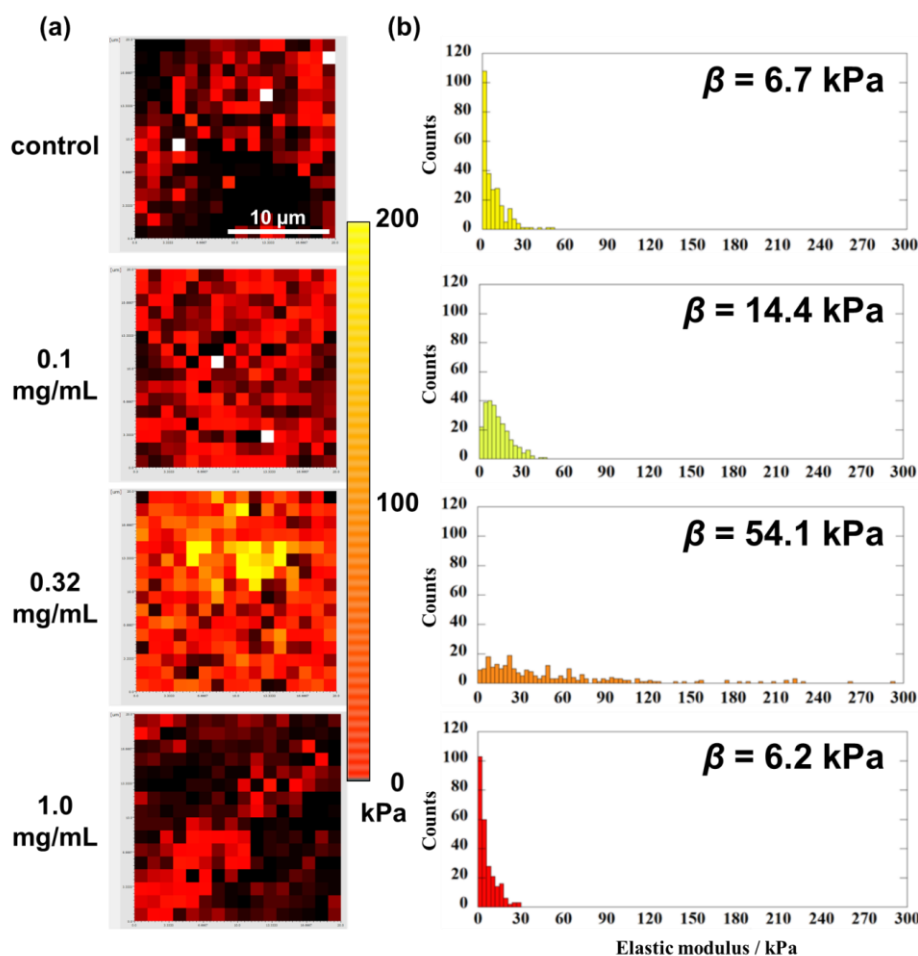

Fig. 8. (a) The results of the Young's modulus mapping are represented as heatmaps for the control (no NRL nanoparticles) and NRL-filled spheroid with NRL nanoparticle concentrations of 0.1, 0.32, and 1.0 mg/mL on day 21, covering an area of 20 x 20 μm². The approach follows the Johnson-Kendall-Roberts (JKR) two-point method. The white areas indicate no data detection. (b) The histogram illustrates the elastic modulus of chondrocyte spheroids at four different NRL concentrations (0, 0.1, 0.32, and 1.0 mg/mL). The median (β) is fitted using the Weibull distribution function. (Copyright 2020. Reproduced from ref. 29).

The adhesion force histogram of the spheroids is shown in Figure 9b. Spheroids cultured without NRL nanoparticles exhibited a broader distribution of forces compared to NRL-loaded spheroids. The evaluated mean adhesion forces were 545 pN and 244 pN for the control and NRL-loaded (0.32 mg/mL) spheroids, respectively. These results is attributed to the interaction of the spheroid's rigid surface structures, as assumed above.

According to previous studies, it has been reported that damage to articular cartilage, which is mechanically inferior to fibrous cartilage, is repaired by the formation of fibrous cartilage[32]. It has been reported that the maximum pressure exerted on human articular cartilage during rising from a chair is estimated to be around 18 MPa[33]. Therefore, articular cartilages are referred to as a viscoelastic tissue and it behaves like the stiff elastic

polymer resistant to sudden impact loading[34]. These findings suggest the need for regenerative tissues of articular cartilage to provide mechanical functionality to withstand high pressures. However, previous studies have not reported the differentiation of human mesenchymal stem cells (hMSCs) into chondrocytes or their sustained effects on the formation of mechanically stable cartilage structures. NRL nanoparticles may play a potential role as a load-bearing component in the repair of cartilage tissue.
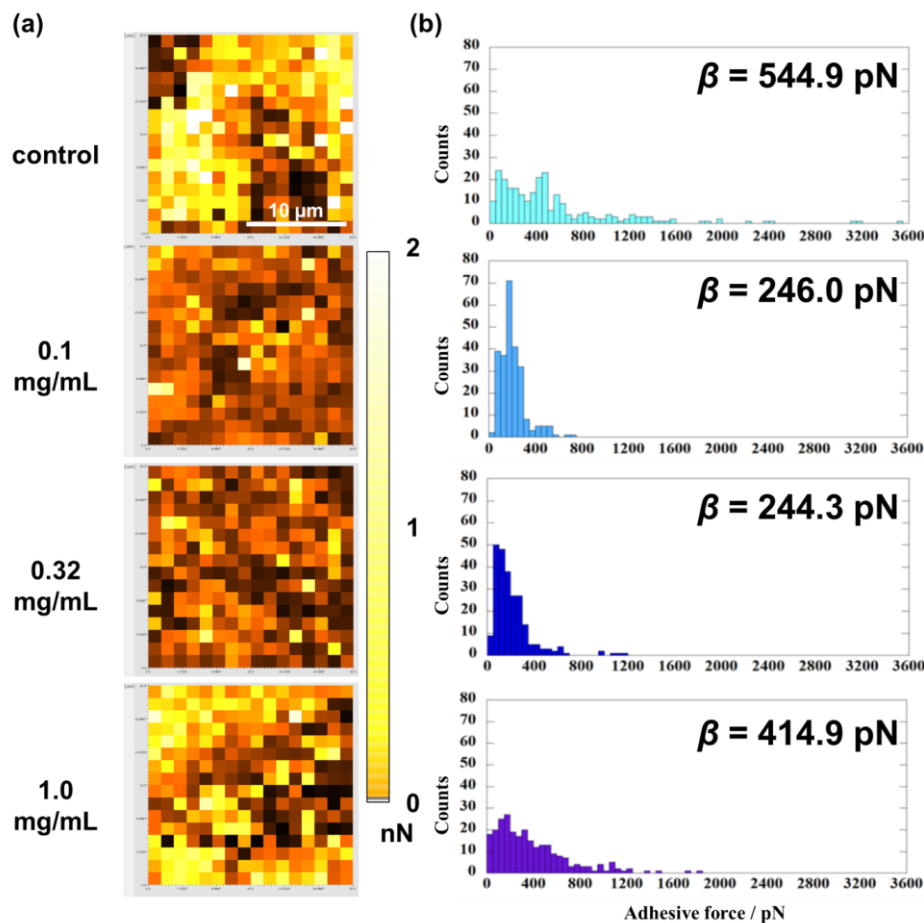

Fig. 9. (a) The results of the adhesion force mapping are presented as heatmaps for the control (no NRL nanoparticles) and NRL-filled spheroid with NRL nanoparticle concentrations of 0.1, 0.32, and 1.0 mg/mL on day 21, covering an area of 20 x 20 µm². The adhesive force is calculated for the unloaded stage and the loaded stage in the contraction curve, focusing on the maximum load point. The white areas indicate no data detection. (b) The histogram illustrates the adhesion force of chondrocyte spheroids at four different NRL concentrations (0, 0.1, 0.32, and 1.0 mg/mL). The median (β) is fitted using the Weibull distribution function. (Copyright 2020. Reproduced from ref. 29).

5. Conclusions

NRL nanoparticles have primarily been used in conventional industrial products, but their target applications are continuously expanding in the field of tissue engineering. In this review, we discussed the cytotoxicity of NRL nanoparticles towards normal (healthy) cells and cancer cells. Currently, furthermore, detailed studies have reported their ability to induce cell cycle arrest and apoptosis profiles[11]. For the knowledge of NRL nanoparticles in tissue engineering and regenerative medicine, Okamoto's group has successfully fabricated cartilage/NRL bio-composite materials through hMSC spheroid formation for the first time. These results indicate a promising future for the application of NRL nanoparticles for tissue engineering. Further efforts are required to investigate the mechanical properties of bio-composite materials and long-term toxicity in a preclinical environment. In tissue engineering and regenerative medicine, the complex interplay between cell and surface structures, as well as the underlying NRL-regulated signal transduction and gene expression during processes such as development, wound healing, and cancer infiltration, will be the focus of future research.

The driving force behind NRL-based tissue engineering is the recognized need for the three pillars of sustainability: environmental by being bioavailable from a natural and renewable source, social by supporting rural communities, and economic by increasing the income of regions dependent on bioproducts. It is time to reflect on this topic and make the research on tissue engineering and regenerative medicine more circular albeit the regulatory challenges.

It is our duty to change the mindset and follow this new trend in which environment, global health and circular economy can be combined.

Conflict of interest
The author declared no competing financial interest.

Author Contributions
The author did all the research work of this study.

References

1   Gurib-Fakim A. Medicinal plants: traditions of yesterday and drugs of tomorrow, *Mol Aspects Med*. 2006; 27(1):1–93.

2   Konno K, Hirayama C, Nakamura M, Tateishi K, Tamura Y, Hattori M, Kohno K. Papain protects papaya trees from herbivorous insects: role of cysteine proteases in latex, *The Plant Journal*. 2004;37(3):370–378.

3   Tang C, Huang D, Yang J, Liu S, Sakr S, Li H, Zhou Y, Qin Y. The sucrose transporter HbSUT3 plays an active role in sucrose loading to laticifer and rubber productivity in exploited trees of Hevea brasiliensis (para rubber tree), *Plant Cell Environ*. 2010;33:1708–1720.

4   Ereno C, Catanzaro Guimaraes SA, Pasetto S, Herculano RD, Silva CP, Graeff CFO, Tavano O, Baffa O, Kinoshita A. Latex use as an occlusive membrane for guided bone regeneration, *J Biomed Mater. Res*. A. 2010;95A:932–939.

5   Herculano RD, Silva CP, Ereno C, Catanzaro Guimaraes SA, Kinoshita A, de Oliveira Graeff C.F. Natural Rubber Latex Used as Drug Delivery System in Guided Bone Regeneration (GBR), *Mater Res*. 2009;12(2):253–256.

6   Sampaio RB, Mendonca RJ, Simioni AR, Costa RA, Siqueira RC, Correa VM, Tedesco AC, Haddad A, Netto JC, Jorge R. Rabbit Retinal Neovascularization Induced by Latex Angiogenic-Derived Fraction: An Experimental Model, *Current Eye Res*. 2010;35(1):56–62.

7   Floriano JF, Silveira da Mota LSL, Furtado EL, Rossetto VJV, Graeff CFO. Biocompatibility studies of natural rubber latex from different tree clones and collection methods, *J Mater Sci: Mater Med*. 2014;25:461–470.

8   Almedia LM, Floriano JF, Ribeiro TP, Mango LN, da Mota LS, Peixoto N, Mrue´ F, Melo-Reis P, Lino Junior Rde S, Graeff CF, Gonçalves PJ. Hancornia speciosa latex for biomedical applications: physical and chemical properties, biocompatibility assessment and angiogenic activity, *J Mater Sci: Mater Med*. 2014;25:2153–2162.

9   Mrué, F. Neoformação tecidual induzida por biomembrana de látex natural com polilisina: aplicabilidade na neoformação esofágica e da parede abdominal. Estudo experimental em cães, Faculdade de Medicina Ribeirão Preto, University of São Paulo, Ribeirão Preto, Brazil, 2000; Accessed October 3, 2023.
    http://dedalus.usp.br/F/N465C3LQTU7JPUHYEV C1P612IH9NXEL7VINQI4SN71IQ2T13E5-33251?func=full-set-set&set_number=000444&set_entry=000008&fo rmat=999.

10 Balabanian CA, Coutinho-Netto J, Lamano-Carvalho TL, Lacerda SA, Brentegani LG. Biocompatibility of natural latex implanted into dental alveolys of rats, *J Oral Sci*. 2006;48(4):201–205.

11 Furuya M, Shimono N, Yamazaki K, Domura r, Okamoto M. Cytotoxicity and anticancer activity of natural rubber latex particles for cancer cells, *Materials Today Chem*. 2017; 5:63–71.

12 Lam KL, Yang KL, Sunderasan E, Ong MT. Latex C-serum from Hevea brasillensis induces non-apoptotic cell death in hepatocellular carcinoma cell line (HepG2). *Cell Prolif*. 2012;45:577–585.

13 Furuya M, Shimono N, Yamazaki K, Domura R. Okamoto M. *e-J Soft Mater*. 2017;12:1–10.

14 Borges FA, de Almeida Filho E, Miranda MC, dos Santos ML, Herculano RD, Guastaldi AC. Natural rubber latex coated with calcium phosphate for biomedical application, *J Biomater Sci Polym Ed*. 2015;26 (17):1256–1268.

15 Butcher DT, Alliston T, Weaver VM. A tense situation: forcing tumour progression. *Nat Rev Cancer*. 2009;9:108-22.

16 Moura JM, Ferreira JF, Marques L, Holgado L, Graeff C.F, Kinoshita A. Comparison of the performance of natural latex membranes prepared with different procedures and PTFE membrane in guided bone regeneration (GBR) in rabbits, *J Mater Sci: Mater Med*. 2014;25:2111–2110.

17 Mendonça RJ, Maurício VB, Teixeira Lde B, Lachat JJ, Coutinho-Netto J. Increased vascular permeability, angiogenesis and wound healing induced by the serum of natural latex of the rubber tree Hevea brasiliensis, *Phytother Res*. 2010;24(5):764–768.

18 Furuya M, Shimono N, Okamoto M. Fabrication of biocomposites composed of natural rubber latex and bone tissue derived from MC3T3-E1 mouse preosteoblastic cells. *Nanocomposites*. 2017;3:76–83.

19 Verron E, Khairoun I, Guicheux J, Bouler JM. Calcium phosphate biomaterials as bone drug delivery systems: A review. Drug Discovery Today.2010; 15(13–14):547–552.

20 Grayson WL, Bunnell BA, Martin E, Frazier T, Hung BP, Gimble JM. Stromal cells and stem cells in clinical bone regeneration.Nature Reviews. *Endocrinology*. 2015;11(3):140–150.

21 Scarfì S. Use of bone morphogenetic proteins in mesenchymal stem cell stimulation of cartilage and bone repair. *World J Stem Cells*. 2016; 8(1):1–12.

22 Singh S, Wu BM, Dunn JC. The enhancement of VEGF-mediated angiogenesis by polycaprolactone scaffolds with surface cross-linked heparin. *Biomaterials*. 2011;32(8):2059–2069.

23 Rosa SSRF, Rosa MFF, Fonseca MAM, Luz GVDS, Avila CFD, Domínguez AGD, Richter VB. Evidence in practice of tissue healing with latex biomembrane: Integrative review. *J Diabetes Research*. 2019:7457295.

24 Frade MA, Assis RV, Coutinho-Netto J, Andrade TA, Foss NT. The vegetal biomembrane in the healing of chronic venous ulcers. *Anais Brasileiros de Dermatologia*. 2012;87(1):45–51.

25 Mendonça RJ, Maurício VB, Coutinho-Netto J. Increased vascular permeability, angiogenesis and wound healing induced by the serum of natural latex of the rubber tree Hevea brasiliensis. *Phytotherapy Research*. 2010;24(5):764–768.

26 Park JS, Yang HN, Woo DG, Jeon SY, Do H-J, Lim H-Y, Kim J-H, Park K-H. Chondrogenesis of human mesenchymal stem cells mediated by the

combination of SOX trio SOX5, 6, and 9 genes complexed with PEI-modified PLGA nanoparticles, *Biomaterials*. 2011;32:3679–3688.

27   Shi D, Xu X, Ye Y, Song K, Cheng Y, Di J, Hu Q, Li J, Ju H, Jiang Q, GuZ. Photo-cross-linked scaffold with Kartogenin-encapsulated nanoparticles for cartilage regeneration, *ACS Nano*. 2016;10:1292–1299.

28   Kinoshita M, Okamoto Y, Furuya M, Okamoto M. Biocomposites composed of natural rubber latex and cartilage tissue derived from human mesenchymal stem cells, *Mater Today Chem*. 2019;12:315–323.

29   Okamoto Y, Kinoshita M, Okamoto M. Fabrication of cartilage/natural rubber latex biocomposites derived from human mesenchymal stem cells in hypoxia, *Nanocomposites*. 2020;6:137–148.

30   Villasante A, Vunjak-Novakovic G. Tissue-engineered models of human tumors for cancer research, *Expert Opin Drug Discov*. 2015;10:257–268.

31   Wang YC, Ludwigson M, Lakes RS. Deformation of extreme viscoelastic metals and composites, *Mater. Sci. Eng A*.2004;370:41–49.

32   Asheesh B, Feeley BT, Williams III RJ. Management of articular cartilage defects of the knee, *J Bone Joint Surg*. 2010;92:994–1009.

33   Hodge WA, Fijan RS, Carlson KL, Burgess RG, Harris WH, Mann RW. Contact pressures in the human hip joint measured in vivo, *Proc Natl Acad Sci USA*. 1986; 83(9):2879–2883.

34   Mow VC, Zhu W, Lai WM, Hardingham TE, Hughes C, Muir H. The influence of link protein stabilization on the viscometric properties of proteoglycan aggregate solution, *Biochim Biophys Acta*. 1989;992(2):201–208.